THE MUON g-2 EXPERIMENT AT BNL

Y. K. SEMERTZIDIS,[a] H. N. BROWN, G. BUNCE, G. T. DANBY, R. LARSEN, Y. Y. LEE, W. MENG, J. L. MI, W. M. MORSE, D. NIKAS, C. OZBEN, C. PAI, R. PRIGL, R. SANDERS, M. TANAKA, D. WARBURTON
Brookhaven National Lab, Upton, New York 11973

R. M. CAREY, W. EARLE, E. EFSTATHIADIS, M. HARE, E. S. HAZEN, F. KRIENEN, J. P. MILLER, O. RIND, B. L. ROBERTS, L. R. SULAK, A. TROFIMOV
Department of Physics, Boston University, Boston, Massachusetts 02215

V. P. DRUZHININ, G. V. FEDOTOVICH, B. I. KHAZIN, I. LOGASHENKO, N. M. RYSKULOV, S. SEREDNYAKOV, Y. M. SHATUNOV, E. SOLODOV
Budker Institute of Nuclear Physics, Novosibirsk, Russia

Y. ORLOV
Newman Laboratory, Cornell University, Ithaca, New York 14853

D. WINN
Fairfield University, Fairfield, Connecticut 06430

A. GROSSMANN, K. JUNGMANN, P. NEUMAYER, G. ZU PUTLITZ, P. V. WALTER
Physikalisches Institut der Universitat Heidelberg, 69120 Heidelberg, Germany

P. T. DEBEVEC, W. DENINGER, F. GRAY, D. W. HERTZOG, C. J. G. ONDERWATER, C. POLLY, S. SEDYKH, M. SOSSONG, D. URNER
Physics Department, University of Illinois at Urbana-Champaign, Urbana-Champaign, Illinois 61801

U. HAEBERLEN
MPI fur Medizinische Forschung, 69120 Heidelberg, Germany

A. YAMAMOTO
KEK, High Energy Accelerator Research Organization, Tsukuba, Ibaraki 305-0801, Japan

P. CUSHMAN, L. DUONG, S. GIRON, J. KINDEM, I. KRONKVIST, R. McNABB, D. MILLER, C. TIMMERMANS, D. ZIMMERMAN
Department of Physics, University of Minnesota, Minneapolis, Minnesota 55455

[a]Presented at the Adrianfest in Honor to Adrian Melissinos' 40 years of service to Physics, Rochester University, September 24-25, 1999.

M. IWASAKI, M. KAWAMURA
Tokyo Institute of Technology, Tokyo, Japan

H. DENG, S. K. DHAWAN, F. J. M. FARLEY, M. GROSSE-PERDEKAMP, V. W. HUGHES, D. KAWALL, W. LIU, J. PRETZ, S. I. REDIN, A. STEINMETZ
Department of Physics, Yale University, New Haven, Connecticut 06511

The construction of the Muon $g-2$ experiment at BNL has finished and the first results towards a final goal of 0.35 ppm are coming out. The pion injection run of 1997 has resulted to a 13 ppm measurement of the anomalous magnetic moment of the muon and the 1998 muon injection run to a 5 ppm. The 1999 run, during which there were collected over two billion events with energy greater than 1.8 GeV, is being analyzed.

1 Introduction

The gyro-magnetic ratio (g-factor) of a particle is defined as the ratio of the magnetic moment, in units of its Bohr magneton, over its angular momentum, in units of $\hbar$:

$$g = \frac{\frac{\text{magnetic moment}}{e\hbar/2mc}}{\frac{\text{angular moment}}{\hbar}} \tag{1}$$

For a Dirac, point-like, spin 1/2 particle the predicted value for $g = 2$. The g-factor of the proton $(+5.587)$ and neutron (-3.826) was found very early to be different from the value appropriate for point-like particles and was the first indication of them being composite particles. The ratio of the proton to neutron g-factors is -1.46 close to that predicted (-3/2) by the constituent quark model.[1]

2 Theory of a_μ

For point-like particles like electrons/positrons, and muons the g-factor is still different from 2 due to quantum field fluctuations. The quantity $a = \frac{g-2}{2}$ is called the anomalous magnetic moment and is the sum of electromagnetic, weak and strong interactions contribution plus any unknown new physics which may be present:

$$a(theo) = a(QED) + a(hadronic) + a(weak) + a(new\ physics) \tag{2}$$

2.1 QED contribution

The electron $\mathrm{g}-2$ experiments are the best laboratory for checking the QED portion of the standard model. The theoretical estimation of the QED part has been carried out to the eighth order [2] with the final accuracy being limited by the accuracy of the fine structure constant. The theoretical value of $a_e(theo) = 1\,159\,652\,153.5(28) \times 10^{-12}$ (24 ppb) is consistent with the measured value [3] of $a(exp) = 1\,159\,652\,188.4(4.3) \times 10^{-12}$ (4 ppb). The difference is $a(theo) - a(exp) = 35(28) \times 10^{-12}$. The most accurate value of α can be obtained by equating the experimental value with the theoretical one:

$$\alpha^{-1} = 137.035\,999\,58(52) \tag{3}$$

It is worth noting that only the photon and electron/positron contributions are probed, with the muon, tau, hadrons, etc., being beyond the current experimental sensitivity of the electron $\mathrm{g}-2$.

The CERN experiments [4,5] have confirmed the $\mu - \mathrm{e}$ universality, i.e. the muons behave like heavy electrons, and the modification of the photon propagator involving virtual hadrons. The QED part of $\mathrm{a}_\mu(\mathrm{QED})$ (figure (1)) is calculated from the equation: [2,6]

$$a_\mu(QED) - a_e(QED) = 1.094\,337\,0(\frac{\alpha}{\pi})^2 + 22.867\,6(33)(\frac{\alpha}{\pi})^3 + \tag{4}$$

$$127.50(41)(\frac{\alpha}{\pi})^4 + 570(140)(\frac{\alpha}{\pi})^5 \tag{5}$$

and using the value of α from Eq. (3) we get: $a_\mu(QED) = 1\,165\,847.06(2) \times 10^{-9}$.

2.2 Hadronic contribution

Even though the electron anomalous magnetic moment at the current experimental sensitivity is only influenced by phons and electrons/positrons, the contribution of heavier particles is important for the muon anomalous magnetic moment. The contribution scales as the mass ratio squared $(m_\mu/m_e)^2 \approx 40,000$. In the muon case the contribution of hadronic vacuum polarization is large, 60 ppm, and cannot be calculated from first principle with the required precision. The contribution in question is depicted in figure (2) and it regards the hadronic content of the photon. This virtual contribution can be estimated exactly by using the optical theorem and the dispersion relation using the hadronic cross section of $\mathrm{e}^+\mathrm{e}^-$ collisions relative to the cross section

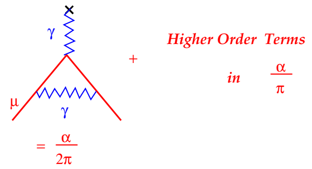

Figure 1: The QED contribution to a_μ.

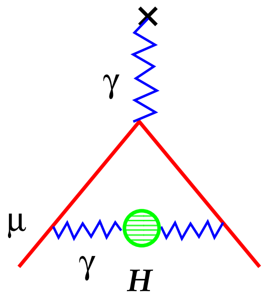

Figure 2: The Hadronic vacuum polarization contribution to a_μ.

of producing $\mu^+\,\mu^-$ pairs (figure (3)). It is not surprising since figure (3) also probes the hadronic content of the photon.

The contribution to a_μ due to the graph of figure (2) is estimated to be

$$a_\mu(had1) = (\frac{\alpha m_\mu}{3\pi})^2 \int_{4m_\pi^2}^{\infty} \frac{ds}{s^2} K(s) R(s) \tag{6}$$

with $R(s) = \frac{\sigma_{tot}(e^+e^- \to hadrons)}{\sigma_{tot}(e^+e^- \to \mu^+\mu^-)}$ and $K(s)$ a kinematic factor going to the value 1 as the center of mass energy squared s goes to infinity. The major contribution to the above integral comes from the low energy resonances below $s = 1GeV^2$ which is extensively being studied by the VEPP-IIM and CMD-II detectors of the Budker Institute for Nuclear Physics in Novosibirsk.[7]

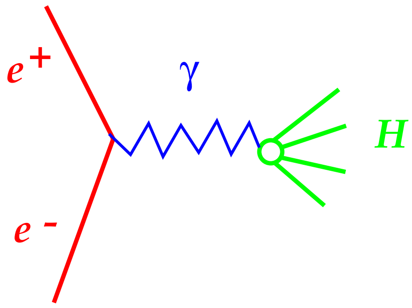

Figure 3: The Hadronic content of the photon is estimated using the cross section of $e^+ e^-$ going to real hadrons.

This hadronic contribution can also be estimated using hadronic τ decays (figure (4)) assuming that conserved vector currents (CVC) holds. The total hadronic contribution is found to be: [8,9]

$$a_\mu(had) = 67.71(77) \times 10^{-9} \ (58.07 \pm 0.66)\text{ppm} \tag{7}$$

2.3 Weak contribution

The week interaction contribution comes from the Feynman graphs which includes virtual Ws and Zs (figure (5)). The W contribution is

$$a_\mu(W) = \frac{G_F m_\mu^2}{8\pi^2\sqrt{2}} \frac{10}{3} = +3.89 \times 10^{-9} \tag{8}$$

and the Z

$$a_\mu(Z) = \frac{G_F m_\mu^2}{8\pi^2\sqrt{2}} \frac{1}{3}[(3 - 4cos^2\theta_w)^2 - 5] = -1.94 \times 10^{-9} \tag{9}$$

The second order contribution has also been estimated and the total effect is [10,11]

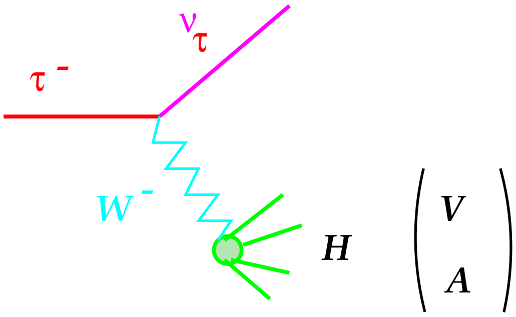

Figure 4: Hadronic τ decays can be used to estimate a_μ.

$$a_\mu(weak) = 1.51(4) \times 10^{-9} \tag{10}$$

The total theoretical estimation of a_μ due to the standard model is

$$a_\mu(theo) = 1\,165\,916.28(77) \times 10^{-9}\ (\pm 0.66\,\text{ppm}) \tag{11}$$

with the error of (± 0.66 ppm) being dominated entirely by the error in the hadronic sector. This error will keep decreasing as new data is becoming available from Novosibirsk and other e^+e^- machines with a low center of mass energy are coming on-line (e.g. Frascatti) or already are collecting data in the interesting region (Beijing).

2.4 Beyond the Standard Model contributions

The contribution from Physics beyond the Standard Model to the muon anomalous magnetic moment is always one of the first hurdles every new model needs

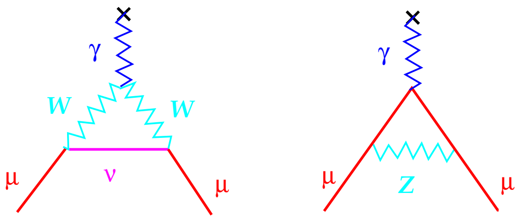

Figure 5: The virtual W and Z contribution to a_μ.

to overcome. In the case of the SUSY with large $\tan\beta$ the muon $g-2$ sets the limits currently which comes from the contribution of the super-symmetric partners of W and Z. This is equal to

$$a_\mu^{\text{SUSY}} \approx \pm 140 \times 10^{-11} [\frac{100\text{GeV}}{M_{\text{SUSY}}}]^2 \tan\beta \tag{12}$$

with M_{SUSY} the SUSY mass scale and $\tan\beta$ the ratio of the vacuum expectation values of the two Higgs doublets. In other models, like SUGRA, [12] there are exclusion area plots (figure (6)) which depend on the masses of the super-symmetric particles.

3 BNL Experiment

A major effort was launched at Brookhaven National Lab towards building the muon $g-2$ experiment starting mid 80s. BNL has available for physics the brightest proton source in the world capable of producing enough muons to make an improvement of a factor of 20 over the last CERN experiment [4,5] in a reasonable time. It was thought that muon injection rather than pion injection into the muon storage ring would be much more efficient and the

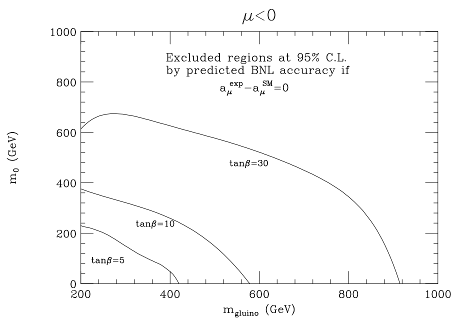

Figure 6: The exclusion area plot assuming the experimental a_μ agrees with the theoretical one to 0.35 ppm for various $\tan\beta$ values.

required investment seems to have paid off. An integral part of this is a pulsed magnetic kicker which delivers enough field to store the muons into stable orbits without on the other hand compromising the B-field quality due to eddy currents.

The construction of the largest super-conducting magnet in the world with the best field uniformity for a big volume was a challenging task which came to a successful conclusion a couple of years ago. The magnetic field had to be roughly a factor of ten better than what was achieved before, a formidable task.

3.1 Principle of $\mathrm{g}-2$

The first muon $\mathrm{g}-2$ experiment was performed in the fifties soon after the parity violation was discovered and a polarized muon source was available. [13] The muon decays to an electron and two neutrinos with the decay being a V-A which violates parity in a maximal way. The average electron momentum in the muon rest frame is along the muon spin direction. Therefore the decay electron angular distribution was used to probe the muon spin direction. In the first experiment there was a muon beam prepared with the spin and momentum originally aligned. This beam was then put through a cyclotron magnet for a fraction of a turn and the angular distribution of the decay electrons relative to the momentum vector was checked again. The relative accuracy on the g-factor was 10%. It was the first time the difference between the spin angle in the muon rest frame and the momentum angle were compared giving rise to the principle of g $-$ 2. It turns out that this same principle holds even for relativistic particles when a complete account of the angle differences are taken, including Thomas precession. A fairly complete account of the g $-$ 2 principle is given by Farley and Picasso. [5] The precession is described by the BMT equation [15] which under certain conditions reduces to

$$\vec{\omega}_a = -\frac{e}{m_\mu}[a_\mu \vec{B} + (\frac{1}{\gamma^2 - 1} - a_\mu)\vec{\beta} \times \vec{E}] \tag{13}$$

which is strictly true only when $\vec{\beta} \cdot \vec{E} = \vec{\beta} \cdot \vec{B} = 0$. The overall experimental technique is described in figure (7).

3.2 Beamline and Inflector

Since neutrinos only come in one handedness one can get naturally polarized muons from pion decays to a muon and a neutrino. This can be done by selecting a small solid angle in the pion rest frame for the decay muon (since direction is related to handedness) and for pions with a kinetic energy of around 3 GeV a momentum bite of 0.5 % is enough to ensure 97% muon polarization.

Figure (8) shows the proton extraction beamline and the target (water cooled disks of Ni). A 24 GeV beam hits the target and a set of quads collects the pions with wide momentum range. The first dispersion point (between D1 and D4 of figure (8)) the pion momentum is selected. The pion decay channel is where the pion decay muons are collected followed by a pion/muon selection slit. The experiment is designed to run either with pion or muon injection into the ring. For the pion injection case about 50% of the pions haven't decayed at the ring entrance. In the muon injection case the fraction of pions (in the pion decay portion of the beamline) contributing to the muon beam is about 38%. About 50,000 muons are stored in the ring every 2.5 s when the primary proton intensity is $40 \times 10^{12}/2.5$ s. All of the data collection in 1998 and most of 1999 were taken in 6 bunches 33 ms apart. Later on the experiment switched to 12 bunches every 33 ms and run up to $60 \times 10^{12}/2.8$ s.
The acceptance of the beamline is $64\,\pi$ mm mrad horizontally and $56\,\pi$ mm mrad vertically. The beam needs to be squeezed through an inflector [16] with dimensions 6 cm high by 1.8 cm wide and 1.7m long. The opening of the inflector is

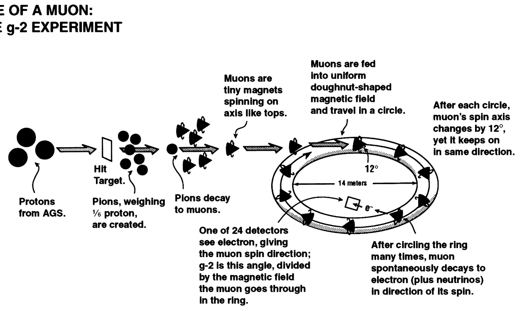

Figure 7: Protons hit a Ni target and produce numerous pions in a wide energy spectrum. A small energy range around 3 GeV of pions is collected into the beamline. Decay muons with a small momentum bite are highly polarized longitudinally. Those muons enter a very uniform vertical dipole magnetic field and precess horizontally. The muon spin precesses slightly faster than the momentum and this angle difference is probed by looking at the muon decay positron energy as a function of time.

77 mm away from the center of the muon storage region.

The inflector's function is to eliminate the main magnet field the injected pions/muons see entering the ring. The design of the inflector was mainly based on the restriction to have very small stray B-field leaked out into the muon storage region. The stray field in the muon storage region is virtually eliminated by using a super-conducting shield around the inflector windings. The temperature of this super-conducting shield is kept above its critical value when the main field is ramped up (1.45 T). Then the shield temperature is lowered to make it super-conducting and the inflector current can now go to its full value. The field in the inflector is now canceled but there is no field leaking out into the muon storage area.[17]

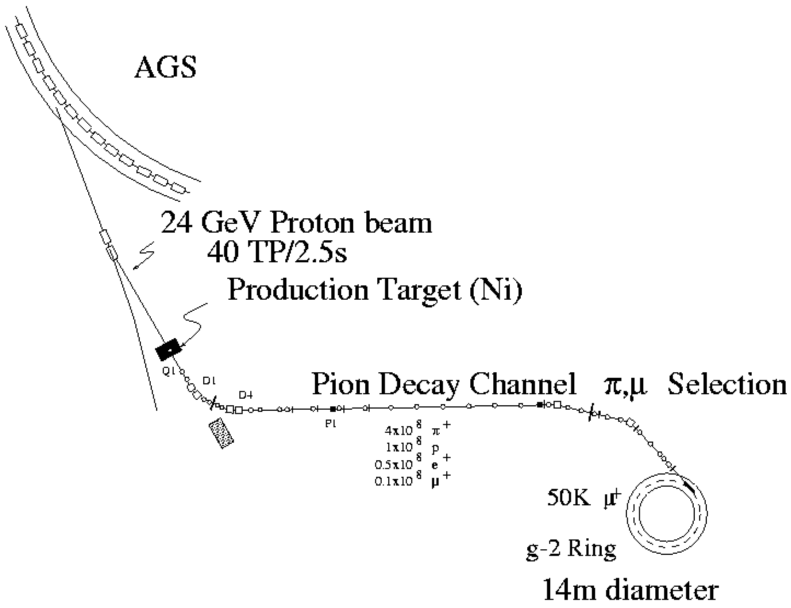

Figure 8: 40×10^{12} protons of 24 GeV energy hit a Ni target every 2.5 s and produce numerous pions in a wide energy spectrum. The protons are distributed in 6 bunches 33 ms apart. A small energy range around 3 GeV of pions is collected into the beamline. About 50,000 muons every 2.5 s are stored in the ring and followed for more than 10 lifetimes ($\tau_\mu \approx 64.4\,\mu$s).

3.3 Magnet

The CERN ring was composed of 40 separate normal conducting magnets [4,14] whereas the current experiment is an iron dominated, single super-conducting magnet. [18] The cross section of the magnet is shown in figure (9) showing the four super-conducting coils, magnet poles, and the muon storage area.

The magnetic field in the muon storage region is measured with NMR probes [19] riding on a beam tube trolley every two to three days. In between the B-field is interpolated using fixed NMR probes located on the top/bottom of the vacuum chambers. The integrated B-field around the azimuth is shown in figure (10) for the 1997 and 1998 run.

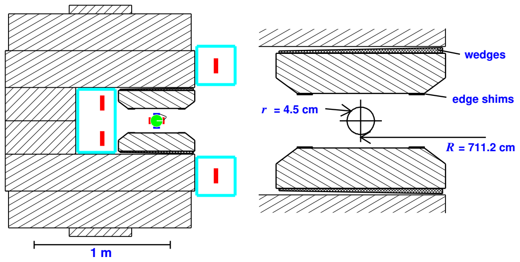

Figure 9: The magnet cross section is shown on the left with the super-conducting coils enclosed in the rectangular boxes. On the right is a closeup of the high quality iron pole pieces and the indication of the muon storage region.

3.4 Electrostatic Quadrupoles and Kicker

Polarized muons are stored in the muon storage ring with vertical focusing provided by an electric quadrupole field. When both electric and magnetic fields are present, the equation for ω_a is given by equation (13).

At the magic gamma, the effect of the electric field on the spin precession frequency and the cyclotron frequency are identical. Hence there is no effect on ω_a. There is a small correction of less than one part per million for off-momentum muons over the 9 cm diameter muon storage region. The muon magic momentum is:

$$p_\mu = \frac{m_\mu}{\sqrt{a_\mu}} = 3.094 GeV/c \tag{14}$$

The electrodes occupied 72% of the total circumference for the CERN experiment. There was a gap at the location of the inflector magnet, which

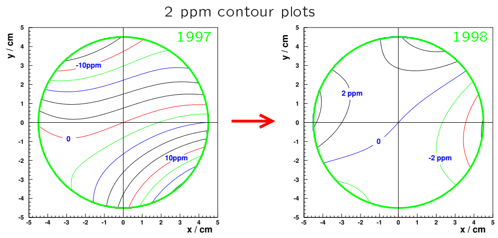

Figure 10: The average magnetic field for the 1997 run (left) and for the 1998 run (right).

cancels the magnetic field for the incoming beam and another gap on the opposite side of the ring to preserve the lattice symmetry. The E821 lattice is shown in figure (11). E821 will be performed with both muon injection and pion injection. Muon injection requires a kicker magnet which kicks the beam onto a stable trajectory. The pion decay provides the kick for pion injection. Muon injection is much more efficient, however. The kicker magnet must be about 90° from the inflector magnet. Therefore space must be left for both the inflector and kicker magnets with two other gaps at 180° and 270° to preserve the lattice symmetry. The electrodes occupy only 43% of the total circumference for the BNL lattice. The electric field gradient must be 1.7 times greater than the CERN design for the same average field index. However, the higher symmetry has two beneficial results: the beta functions are much more uniform around the azimuth and the orbit stability is better.

The NMR beam tube trolley rails and the cross section of the electrostatic quads is shown in figure (12). Since the mixing of the magnetic and electric (non-uniform) fields inevitably produces regions with trapped electrons there was great care to reduce their effects. The last CERN experiment pulsed the quads [20] to reduce the problem due to the accumulated space charge. In the current experiment there were additional design improvements to further reduce the amount of trapped charge [21,22]. The feeding leads on the quad plates were placed in a way to quench the electron trapping and carry the charge all the way outside the muon storage region where it was inevitably lost on the vacuum chamber walls. Even though the E-field gradient was by a factor of 1.7 higher than that of the last CERN experiment the requirements on the vacuum pressure are by more than a factor of ten relaxed in the current experiment at BNL due to those improvements.

The kicker device (3 modules 1.7 m long each) needs to reduce the magnetic field the muons see for very short time. This will put the muons into stable orbits and increase the acceptance of the ring substantially. Also the injected particles into the ring are by a factor of one hundred less for roughly ten times the stored muons for the same primary proton intensity on target. The light flash on the detectors, especially those at the first third of the ring, is reduced considerably. The kicker, however, creates a fast changing magnetic field which creates eddy currents with stray B-field in the muon storage region. This effect was studied and the kicker plates were design in the way to make the eddy current field negligible. The kicker pulse creates about 150 Gauss of peak field with the eddy current B-field being less than 0.1 ppm of the integrated total field by $20\,\mu$s, i.e. negligible. [23]

4 Pion and Muon Injection Runs and Data Analysis

In 1997 we had our first run with pion injection. All the systems in the experiment were commissioned and learned a great deal about the relevant issues under running conditions. About 20 M decay positrons were collected above 1.8 GeV energy were collected in about four week period. Of those roughly 11 M were used in the analysis and the results were published. [24] In August 1998 we had first muon injection run which ended prematurely due to a beam-line magnet failure. There were about 100 M positrons with energy greater than 1.8 GeV collected 75 M of which were used in the analysis. The preliminary analysis of this data set is finished. In 1999, in a 7 week run period we have collected about 2 B positrons with energy greater than 1.8 GeV. The analysis of this data set is on-going. A small fraction of this data set is shown in figure (13).

The 1998 data analysis was separated into four major tasks:

1. Data Production (or Reduction) from raw data
2. ω_a analysis (g-2 muon spin precession frequency analysis)
3. Systematics of ω_a analysis
4. ω_p analysis (NMR analysis of the muon storage region B-field) and its systematics

The main philosophy in the analysis was to get familiar with the data by looking at them in many different ways and challenging the "current" understanding of the various systems of the experiment leaving behind no unexplained "mysteries".

The progress of the analysis was reported on a weekly basis in the offline meetings at BNL and on a daily basis more informally. This ensured adequate feedback and dissemination of information in a very efficient way. At no time the people working on ω_a knew the offset on ω_p and vice versa. This "blind" analysis ensured that there was no bias in making crucial selections.

4.1 Systematics of ω_a analysis

All possible systematic errors have been adequately addressed in internal $\mathrm{g}-2$ notes. The principle things considered in the ω_a analysis were:

1. Background in the data (e.g. flashlets, narrow pulses, quad sparking).
2. Pileup, i.e. the overlap of more than one positron in a single detector influencing the pulse parameters.
3. Muon losses, Gain and Timing stability.
4. Fitting function and method, χ^2.
5. Corrections, like the electric field and pitch. Those corrections are applied to ω_a after the final number is estimated.
6. Fast Rotation (cyclotron frequency), Coherent Radial Motion.

4.2 Results

The function used to fit the data was the exponential decay modulated by the $\mathrm{g}-2$ frequency: $N_0 e^{-t/\tau}[1 + A\cos(\omega_a t + \phi)]$ with a typical normalized $\chi^2 = 1.02$ for roughly 3350 d.o.f. when all the detectors are combined together and the start of the fit is around 40μs (for a total of about 72 M fitted positrons).

All the systematics have been addressed adequately giving a total systematic error (including the ones on the magnetic field) of 1 ppm for the 1998 data. The statistical error of the 1998 data was 5 ppm. The results are shown in figure (14). The anomalous magnetic moment is given by the equation:

$$a_\mu = \frac{R}{\lambda - R} = 0.0011569191(59)\ (5ppm) \tag{15}$$

with $\lambda = \mu_\mu/\mu_p = 3.183\,345\,13(39)$ from the measurement of the Zeeman hyperfine transitions in the ground state of muonium.[25] R is the ratio of the average muon g $-$ 2 frequency over that of the NMR frequency of the free proton averaged over the muon storage region: ω_a/ω_p.

4.3 Future Prospects

The muon g $-$ 2 experiment is expected to run for another two years to reach 0.35 ppm. For the future use of the ring there are two ideas in the Letter of Intent status. The first one aims to probe the muon Electric Dipole Moment at the $10^{-24}\,\mathrm{e}\cdot\mathrm{cm}$ level using a new technique. It utilizes a radial E-field to freeze the muon spin precession in the horizontal plane along the muon momentum. If there is a muon EDM the motional electric field (due to the vertical magnetic field there is a strong motional E-field in the muon rest frame) the spin will precess vertically. This will push the current muon EDM limit by almost six orders of magnitude from the current limit making it very competitive with the electron and neutron EDM. The second one uses the ring as a very uniform spectrometer to reduce the current limit of the muon neutrino mass by roughly a factor of 20 to about 8 KeV.

References

1. Modern Theories of Nuclear Moments by B. Castel and I. S. Towner, (Clarendon Press, Oxford, 1990), p. 4.
2. T. Kinoshita and W.J. Marciano, in Quantum Electrodynamics, Edited by T. Kinoshita (World Scientific, Singapore, 1990), p. 419 and references therein.
3. R.S. Van Dyck, Jr., P.B. Schwinberg, and H.G. Dehmelt, Phys. Rev. Lett. **59**, 26 (1987); R.S. Van Dyck, Jr.in Quantum Electrodynamics, edited by T. Kinoshita (World Scientific, Singapore, 1990), p. 322.
4. J. Bailey, *et al.*, Nucl. Phys. **B150**, 1 (1979).
5. F.J.M. Farley and E. Picasso, in *Quantum Electrodynamics*, edited by T. Kinoshita (World Scientific, Singapore, 1990), p. 419.
6. D. Decamp, *et al.*, Phys. Lett. **246B**, 306 (1990).

7. L.M. Barkov, *et al.*, Nucl. Phys. **256**, 356 (1985); V.M. Aulchenko, *et al.*, Nucl. Inst. Meth. **A252**, 299 (1986), Novosibirsk Preprint INP 85-118 CMP-2 Detector for VEPP-2M.
8. R. Alemany, M. Davier, and A. Hocker, Eur. Phys. J. **C 2**, 123 (1998).
9. M. Davier and A. Hocker, Phys. Lett. **B 419**, 419 (1998) and references therein.
10. A. Czarnecki, B. Krause, and W. Marciano, Phys. Rev. Lett. **76**, 3267 (1996).
11. A. Czarnecki, B. Krause, and W.J. Marciano, Phys. Rev. Lett. **52**, R2619 (1995).
12. U. Chattopadhyay and P. Nath, Phys. Rev. **D 53**, 1648 (1996).
13. R.L. Garwin, L. Lederman, and M. Weinrich, Phys. Rev. **105**, 1415 (1957).
14. H. Drumm, C. Eck, G. Petrucci, and O. Runolfsson, Nucl. Instrum. and Meth. **158**, 347 (1979).
15. V. Bargmann, L. Michel and V. L. Telegdi, *Phys. Rev. Lett.,* **2**, *435 (1959).*
16. *F. Krienen, D. Loomba, and W. Meng, Nucl. Instrum. Methods Phys. Res., Sect. A* **394**, *349 (1997).*
17. *G. T. Danby, W. Meng, W. B. Sampson, K. Woodle, "Magnetic Flux Shielding for the Precision Muon* $\mathrm{g}-2$ *Storage Ring Superconducting Inflector", IEEE Trans. Magnetics* **30**, *1766, 1994.*
18. *G. Danby, et al., "The Brookhaven Muon Storage Ring Magnet", to be submitted to* Nucl. Instrum. Methods *A.*
19. *R. Prigl, et al., Nucl. Instrum. Methods Phys. Res., Sec. A* **374**, *118 (1996).*
20. *W. Flegel and F. Krienen, Nucl. Instrum. and Methods* **113**, *549 (1973).*
21. *G. Bennett, R. Larsen, W. Morse, Y. Semertzidis, J. Yelk, Z. Liu, IEEE Particle Accelerator Conference (PAC 93), Vol. 3, p. 2070-2072, Washington, DC, 17-20 May 1993.*
22. *Y. Semertzidis, et al., "The Muon* $\mathrm{g}-2$ *Storage Ring High Voltage Quadrupoles" to be submitted to* Nucl. Instrum. Methods *A.*
23. *E. Efstathiadis, et al., "The Muon* $\mathrm{g}-2$ *Kicker: Specifications and Performance of the Final Prototype" to be submitted to* Nucl. Instrum. Methods *A.*
24. *R.M. Carey, et al.,* Phys. Rev. Lett.**82**, 1632 (1999).
25. W. Liu, *et al., Phys. Rev. Lett.***82**, *711 (1999).*

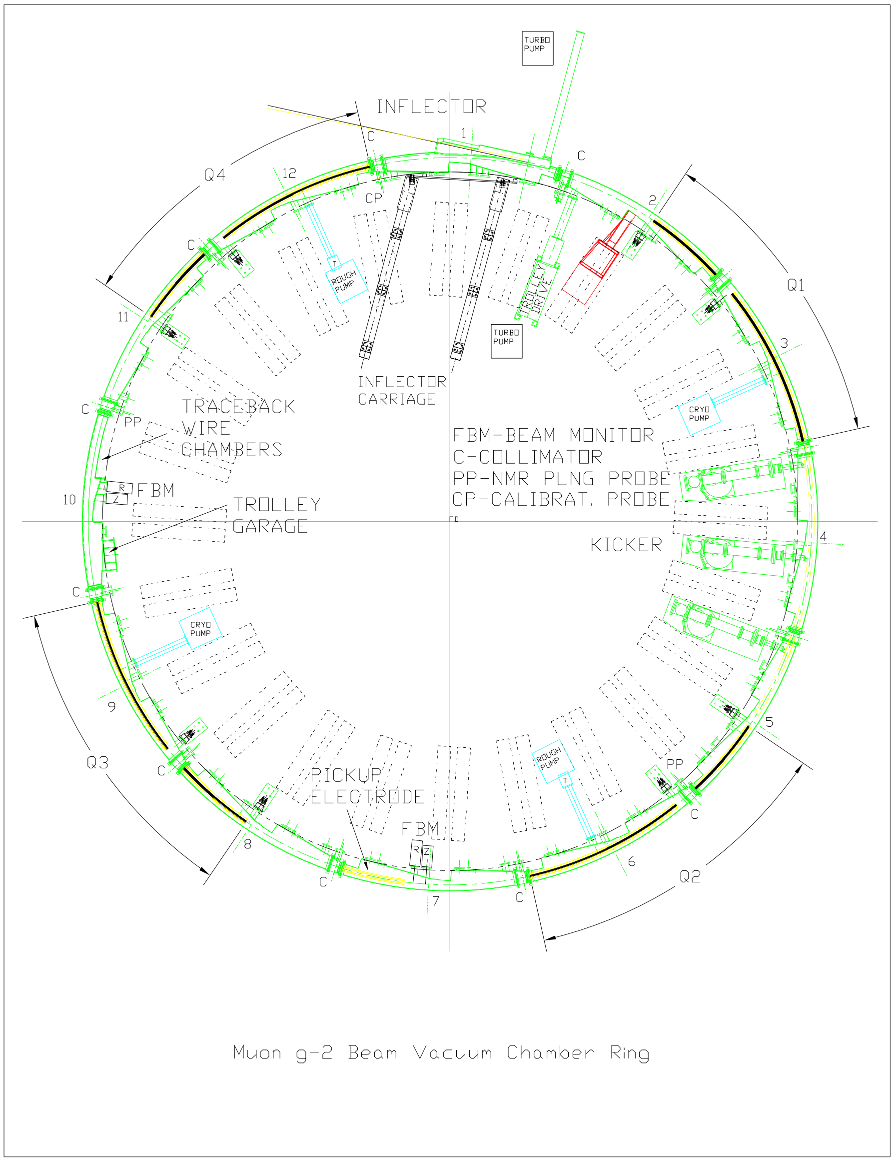

Figure 11: The g − 2 ring (top view). The quadrupole as well as the kicker and detector location is shown.

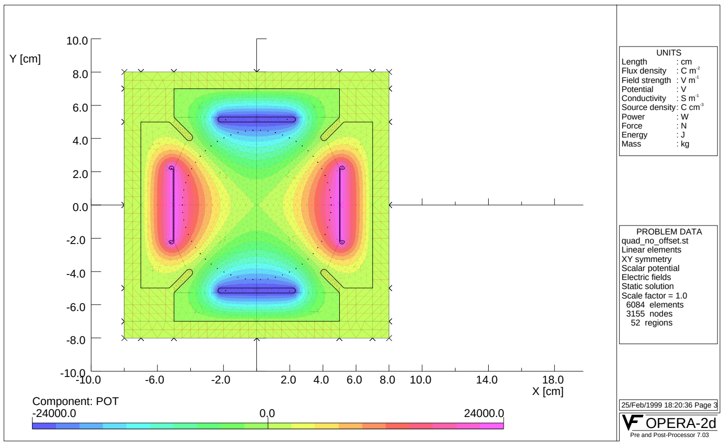

Figure 12: The electrostatic quadrupole cross section. The trolley rails, the voltage equipotential lines and the circular muon storage region of 9 cm in diameter are also shown.

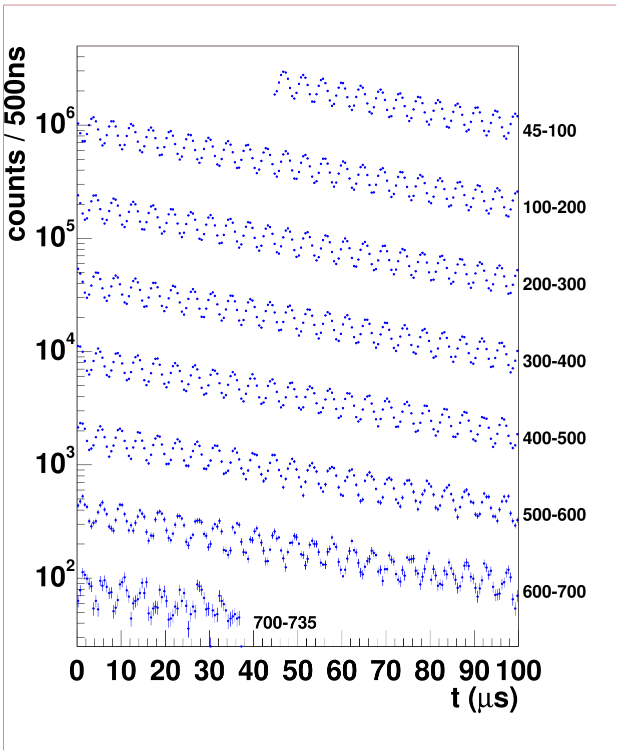

Figure 13: 357 M positrons with E > 1.8 GeV, a small fraction of the 2 B collected in the 1999 run.

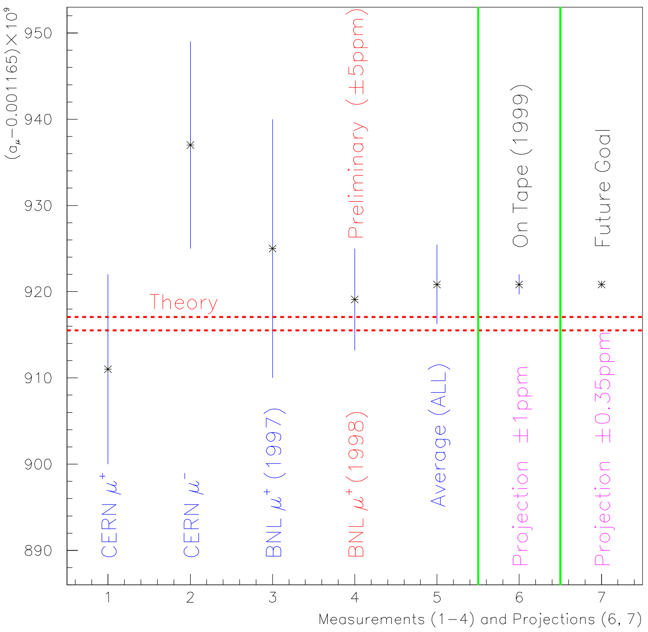

Figure 14: The previous CERN results, the Standard Model prediction and the results from the current experiment are shown $(1 - 4)$. Also shown is the expected error reduction with the conclusion of the 1999 data analysis (6) and with more data collection (7).